DOI 10.24425/aee.2023.146039

Effect of selected parameters on the electrical strength of a high-voltage vacuum insulation system

MICHAŁ LECH ✉, PAWEŁ WĘGIEREK

Faculty of Electrical Engineering and Computer Science, Lublin University of Technology
Nadbystrzycka 38A str., 20-618 Lublin, Poland
e-mail: {✉m.lech/p.wegierek}@pollub.pl

(Received: 09.09.2022, revised: 27.02.2023)

Abstract: The article presents the results of laboratory measurements of U_d breakdown voltages in a high-voltage vacuum insulating system for different pressures, contact gaps, type of electrode contacts and type of residual gas inside the discharge chamber. First of all, the electrical strength of the discharge chamber with a contact system terminated with contact pads made of $W_{70}Cu_{30}$ and $Cu_{75}Cr_{25}$ material was compared for selected values of contact gaps. It was found that below a pressure of $p = 3.0 \times 10^{-1}$ Pa the electrical strength reaches an approximately constant value for each of the set contact gaps d. Analytical relationships were determined to calculate this value for each of the contact pads used. Above a pressure of $p = 3.0 \times 10^{-1}$ Pa, the measured values of U_d breakdown voltages decrease sharply. The values of breakdown voltages in the discharge chamber with residual gases in the form of air, argon, neon and helium were also determined for selected values of contact gaps d. Depending on the residual gases used, significant differences were noted in the values of pressure p at which the loss of insulating properties in the discharge chamber occurred. These values were 3.3×10^{-1} Pa for argon, 4.1×10^{-1} Pa for air, 6.4×10^{-1} Pa for neon, and 2.55×10^{0} Pa for helium, respectively.

Key words: electrical breakdown, electrical contacts, electrical strength, switchgear, vacuum insulation

1. Introduction

Electrical discharge in a gaseous medium involves the flow of electric current through the gas [1]. Considering a classical insulating system consisting of flat electrodes, parallel to each other, to which a regulated voltage source is connected, after exceeding a certain value of it, the kinetic energies of electrons and ions in the interstitial space reach critical values [2]. Above these

values, collisional ionization of inert gas molecules is possible, and thus the onset of avalanche discharge.

In the advanced stage of development of an electric discharge in a gaseous medium, its course depends on many factors [3]. We are talking about, among others, the coefficient of inhomogeneity of the electric field, the contact gap, the pressure and type of gas, or the polarity and voltage change over time. So far, two main mechanisms of gas discharge development have been distinguished: the Townsend mechanism and the channel mechanism. The former occurs for products of pressure p and contact gap d in the range $(10^4 \div 10^5)$ Pa·cm. The channel mechanism, in turn, is divided into two varieties: streamer and streamer-lead. The former occurs for a product of pd in the range $(10^5 \div 10^7)$ Pa·cm, while the latter occurs for a product of pd whose value exceeds 10^7 Pa·cm.

In the case of media in which the pressure is lowered below the value of 10^{-1} Pa, and thus a high vacuum condition is obtained, the mechanisms described above do not apply. Under such conditions, the initiation and development of the discharge follows vacuum mechanisms [4].

Between the pressure value of 10^{-1} Pa and the lower limit of the occurrence of the Townsend mechanism, the development of the discharge is affected by both the phenomena occurring in vacuum mechanisms and the Townsend mechanism.

In the case of vacuum media, when the pressure inside the discharge chamber is reduced to a value at which the average free paths of electrons and molecules have greater values than the contact gap, the probability of electron avalanches developing is significantly reduced. This is the idea of using vacuum as an insulating medium in modern switching apparatus.

The value of the average free path of molecules and electrons in the selected gas can be calculated using the following relationships [5]:

$$L_m = 3.11 \cdot 10^{-24} \frac{T}{p d_m^2}, \tag{1}$$

$$L_e = 1.76 \cdot 10^{-23} \frac{T}{p d_m^2}, \tag{2}$$

where: L_m is the average free path of molecules in the gas, L_e is the average free path of electrons in the gas, T is the absolute temperature of the gas, p is the pressure of the gas, d_m is the diameter of a gas molecule.

If the calculated values of the average free paths of molecules and electrons are greater than the set contact gaps, the electron in the electrode space travels unhindered to the anode, thus preventing the development of an electron avalanche. By measuring the breakdown voltage in systems of this type, it can be seen that the electrical strength in this case, however, has a finite value. The prerequisite for the development of a discharge in a vacuum insulating system is the introduction of electric charge carriers into the interelectrode space, as well as the appearance of a sufficient number of molecules or gas vapors, which ionized will cause the current to rise to short-circuit conditions. The initiation of an electrical breakdown in this situation is influenced by more than a dozen physical phenomena, as shown in Fig. 1.

Focusing on the basic physical phenomena necessary for secondary phenomena and the development of a discharge in a vacuum, four main groups of hypotheses for the mechanisms of initiation and development of discharges in this type of insulating systems have been identified so far:

– It has been hypothesized that there is an inter-electrode exchange of charged particles that arise from secondary emissions [6]. When this exchange becomes cumulative, an electrical breakdown occurs.
– Hypotheses involving field emission of an electron beam from a microstrip or inclusion on the cathode, bombarding the anode [7]. This results in a local increase in the temperature of the anode, thereby releasing gases or vapors in which the discharge develops.
– Hypotheses that assume the movement of charged microparticles between electrodes [8]. The development of the discharge takes place in pairs of material triggered by the impact of the microparticle on the electrode.
– Hypotheses that there is a layer of adsorbed gases on the surfaces of electrodes and the surfaces of the insulating system (such as the discharge chamber) [9]. The development of the electrical discharge takes place in the gases that are desorbed from these surfaces.

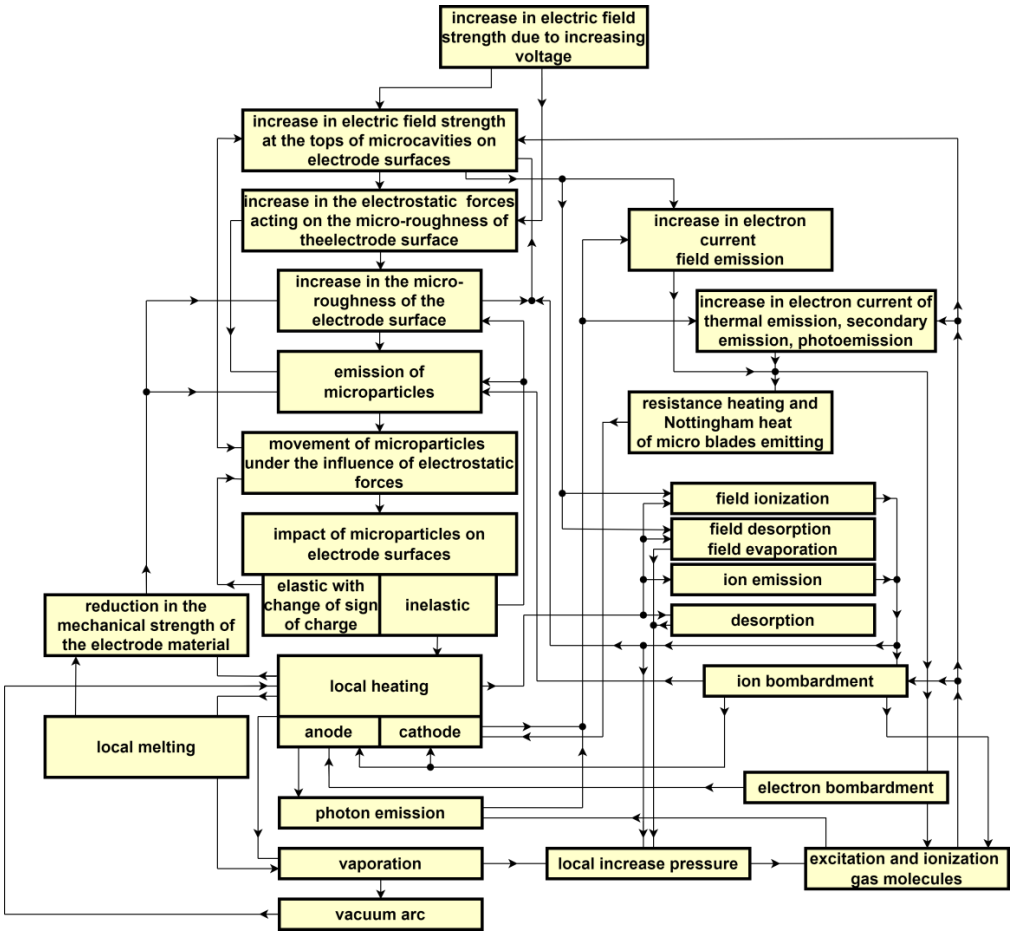

Fig. 1. Physical phenomena and their interaction in the initiation and development of an electrical breakdown in a vacuum insulation system (own elaboration based on [1,4])

The authors of this paper decided to study the effect of selected noble gases (argon, neon and helium) on the strength of a vacuum insulation system. Noble gases are elements from the 18th group of the periodic table of elements. They are present in the Earth's atmosphere in small quantities. They have much lower boiling and melting points compared to other substances of similar atomic or molecular weight [10].

Noble gases, due to their filled valence shells, are extremely stable. They are characterized by high ionization energies, making it difficult to detach an electron from an element's atom. As the group of an element decreases, the atomic radius increases and the ionization energy decreases. Of the gases studied, helium has the highest energy of first ionization (2 370 kJ/mol), while argon has the lowest (1 520 kJ/mol). A summary of the basic properties of the noble gases used in the study is summarized in Table 1.

Table 1. Properties of selected noble gases [10]

Type of gas	**Electron configuration**	**Atomic Radius**	IE_1	EA	**Density at STP**
		pm	kJ/mol	kJ/mol	g/L
He	$1s^2$	32	2 370	+20	0.18
Ne	[He] $2s^2 2p^6$	70	2 080	−30	0.90
Ar	[Ne] $3s^2 3p^6$	98	1 520	+35	1.78

Previously published scientific papers on the analysis of the electrical strength of vacuum insulation systems have mainly used DC voltage test sets and combined systems – DC voltage and AC voltage [11–14]. They presented the results of laboratory measurements of breakdown voltages, focusing on the physical issues of the development of discharges in vacuum. These works analyzed the electrical strength of insulating systems for a range of pressures covering the "bottom" of the Paschen curve and its right and left branches. The authors of this paper focused on the lower pressures for which the electrical strength of the insulating system maintains a constant, safe value, and then compared the pressures at which the insulating properties are lost. The study used an AC test set with a mains frequency of 50 Hz, making the results of this study relevant to industrial applications involving vacuum switchgear.

When analyzing contact materials used in vacuum insulation systems, the main focus should be on vacuum interrupters used in electric power switching equipment. W–Cu and Cu–Cr materials are often used in this type of equipment.

W–Cu material is a bimetallic composite, which is characterized by high hardness and strength, a low coefficient of thermal expansion, and good arc resistance. Composites of this type are mainly used in the manufacture of electrical contacts in electrical equipment, welding electrodes, or heat sinks. They are also widely used in the aerospace industry [15–20].

Contact materials made of Cu–Cr alloys are widely used in medium and high-voltage vacuum interrupters. The good properties of such materials are a resultant of the use of copper and chromium. Copper, with its lower melting point and better conductivity and ductility than chromium, which has higher mechanical strength, makes the end result an alloy with high current carrying capacity and resistance to the negative effects of arc burning [21–25].

The very good physical properties and popularity of the contact materials described above became the authors' motivation for conducting the research presented in this paper. This work shows a new look at vacuum insulation systems, from the point of view of modern switchgear. The results of the authors' research are aimed primarily at designers and manufacturers of vacuum switchgear, who care about increasing the reliability of equipment.

2. Laboratory bench

The laboratory bench used in the described tests of the electrical strength of the vacuum insulation system consists of a high-voltage test set, a discharge chamber with a contact system mounted inside, a set of vacuum pumps with accessories, and a set of technical gases. A block diagram of the test stand is shown in Fig. 2.

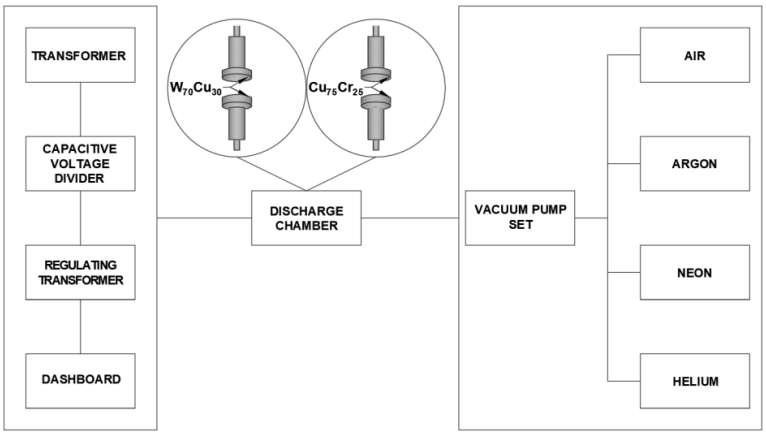

Fig. 2. Block diagram of a laboratory station designed to test the electrical strength of a vacuum insulation system

The main component of the laboratory bench is a discharge chamber designed and constructed in a "demountable" manner. Inside it is mounted a contact system with the possibility of access to it by the person performing the tests. This makes it possible to change electrodes and study the influence of selected material parameters on the arc processes occurring in vacuum media. The adjustment of the contact gap was realized thanks to a system consisting of a DC motor with a gearbox and a linear distance meter with a display. The adjustment process is completely safe for the test person due to the use of a remote control isolated from the bench, allowing precise adjustment of the selected contact gap.

A vacuum set-up, which includes a rotary pre-pump and a turbomolecular pump, is used to ensure adequate pressure inside the discharge chamber. Pressure measurement in the system is carried out using two measuring heads (vacuum gauges), connected to a dedicated display. Dosing of air or selected technical gases into the system is possible thanks to a precise manual valve. A view of the main component of the stand – the discharge chamber with a set of vacuum

pumps and a set of technical gases is shown in Fig. 3(a), while a view of the electrode array inside the discharge chamber is shown in Fig. 3(b).

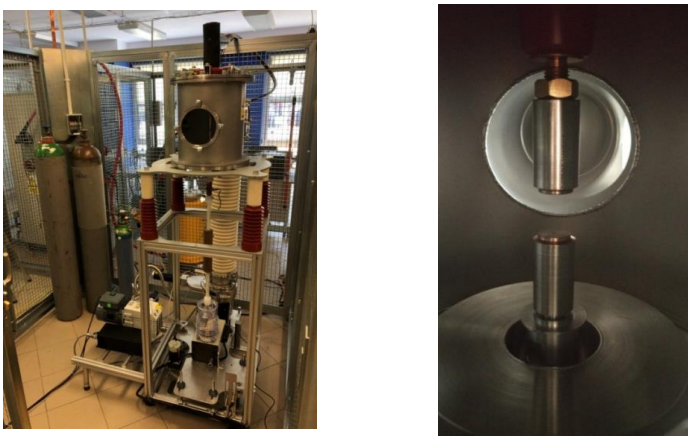

(a) (b)

Fig. 3. (a) View of the main component of the laboratory bench – the discharge chamber with a set of vacuum pumps and a set of technical gases; (b) view of the electrode array inside the discharge chamber

The laboratory bench was powered by a high-voltage test transformer with a rated voltage of 100 kV and a continuous power of 50 kVA, a measuring divider made of low-loss polypropylene capacitors, a regulating autotransformer and a control panel equipped with complete control, protection, signaling and measuring equipment [26]. A view of the complete set supplying the test system is shown in Fig. 4.

(a) (b)

Fig. 4. View of the power supply set: (a) high-voltage test transformer with measuring divider, (b) autotransformer regulator with control panel

3. Results of laboratory tests carried out

3.1. Effect of contact material type on electrical strength

To study the effect of the type of contact material on the electrical strength of the vacuum insulation system, U_d breakdown voltages were measured for two contact materials:

– $W_{70}Cu_{30}$ – copper-filtered tungsten in the ratio: 70% tungsten, 30% copper,

– $Cu_{75}Cr_{25}$ – copper-chromium composite in the ratio: 75% copper, 25% chromium.

Six values of contact gaps selected: $d_1 = 0.7$ mm, $d_2 = 0.9$ mm, $d_3 = 1.5$ mm, $d_4 = 1.7$ mm, $d_5 = 2.3$ mm, $d_6 = 2.7$ mm, and a pressure range (3.0×10^{-3} Pa÷1.0×10^{0} Pa). The obtained measurement results are presented in the form of $U_d = f(p)$ characteristics in Fig. 5(a) and 5(b).

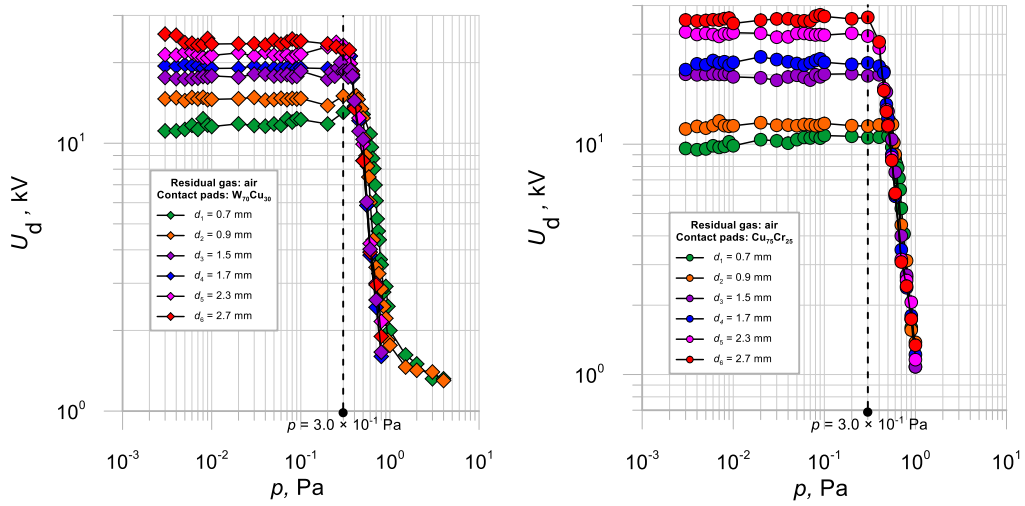

Fig. 5. Dependence of the breakdown voltage U_d as a function of pressure p in the discharge chamber for contact gaps $d_1 \div d_6$: (a) for $W_{70}Cu_{30}$ contacts; (b) for $Cu_{75}Cr_{25}$ contacts

Note the two characteristic ranges of the presented characteristics. The limiting point is a pressure of $p = 3.0 \times 10^{-1}$ Pa, marked in the figures above. For pressures less than this value, the electrical strength reaches an approximately constant value for each of the set contact gaps. Moreover, as the contact gap d increases, the value of the breakdown voltage U_d also increases. The described relationships are valid for both the system with $W_{70}Cu_{30}$ contacts and $Cu_{75}Cr_{25}$ contacts. For pressures greater than the value of $p = 3.0 \times 10^{-1}$ Pa, the electrical strength of the system decreases rapidly, which means that the system loses its insulating capacity. However, these pressure values are not of interest to the authors of this paper, due to the lack of applicability in the field of electrical switching equipment. Analyzing the pressure interval (3.0×10^{-3} Pa $\div$ 3.0×10^{-1} Pa) more meticulously, the characteristics of $U_d = f(d)$ were developed for selected 19 pressure values $p_1 \div p_{19}$, which are shown in Fig. 6(a) and 6(b).

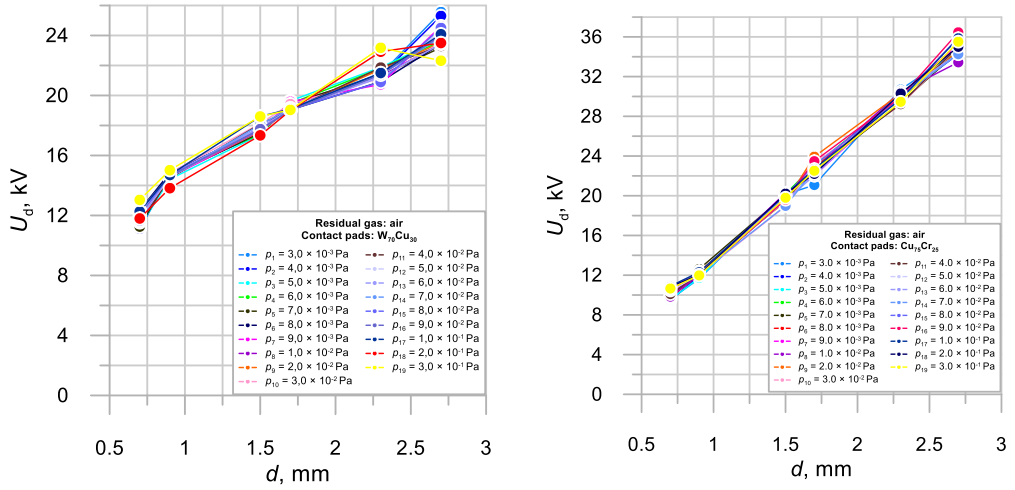

Fig. 6. Dependence of the breakdown voltage U_d as a function of contact gaps d for selected pressure values $p_1 \div p_{19}$: (a) for $W_{70}Cu_{30}$ contacts; (b) for $Cu_{75}Cr_{25}$ contacts with drawn final fitting curves

It was noted that these functions take the form of linear functions of the form $y = Ax+B$. Thus, the fitting curves were determined for each of the pressure values in the interval $p_1 \div p_{19}$, followed by the average values of the coefficients A and B and the final formulas of the fitting functions. The results of the calculations are summarized in Table 2 and 3, while the characteristics of $U_d = f(d)$ with the final fitting functions drawn in are shown in Fig. 7(a) and 7(b).

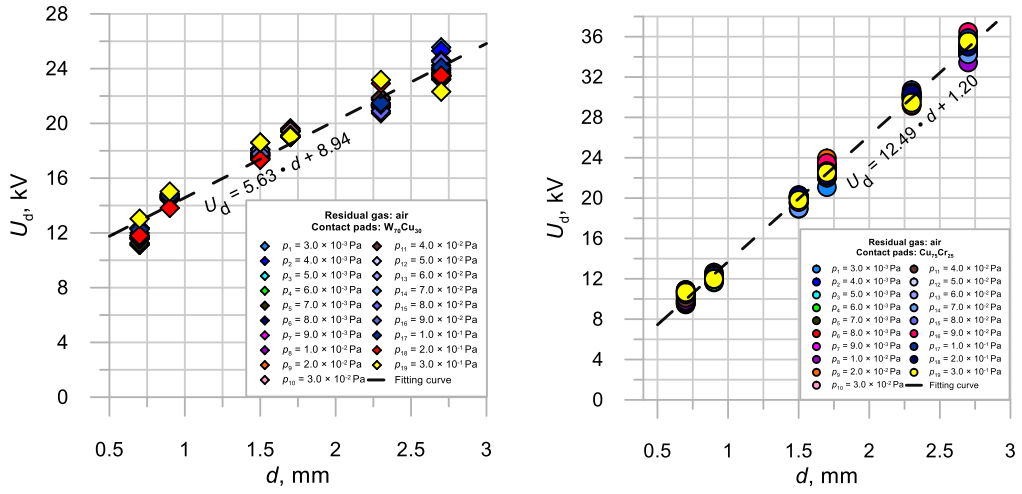

Fig. 7. Dependence of the breakdown voltage U_d as a function of contact gaps d for selected pressure values $p_1 \div p_{19}$: (a) for $W_{70}Cu_{30}$ contacts; (b) for $Cu_{75}Cr_{25}$ contacts

Table 2. Calculation of the final pattern of the fitting curve for contact material $W_{70}Cu_{30}$

Contact material: $W_{70}Cu_{30}$					
Lp.	***p*, Pa**	**Curve fitting pattern**	**A-factor**	**B-factor**	**R^2**
1	3.0×10^{-3}	$y = 6.4305310 \cdot x + 7.7901327$	6.43	7.79	0.96
2	4.0×10^{-3}	$y = 6.2893805 \cdot x + 7.9473451$	6.29	7.95	0.96
3	5.0×10^{-3}	$y = 5.9128319 \cdot x + 8.3957080$	5.91	8.40	0.96
4	6.0×10^{-3}	$y = 5.6256637 \cdot x + 8.9414159$	5.63	8.94	0.97
5	7.0×10^{-3}	$y = 5.5353982 \cdot x + 8.8588496$	5.54	8.86	0.95
6	8.0×10^{-3}	$y = 5.1283186 \cdot x + 9.6770796$	5.13	9.68	0.98
7	9.0×10^{-3}	$y = 5.8000000 \cdot x + 8.6600000$	5.80	8.66	0.96
8	1.0×10^{-2}	$y = 5.5212389 \cdot x + 8.9353097$	5.52	8.94	0.97
9	2.0×10^{-2}	$y = 5.5477876 \cdot x + 9.0119469$	5.55	9.01	0.98
10	3.0×10^{-2}	$y = 5.4300885 \cdot x + 9.2475221$	5.43	9.25	0.95
11	4.0×10^{-2}	$y = 5.5933628 \cdot x + 8.9208407$	5.59	8.92	0.97
12	5.0×10^{-2}	$y = 5.7327434 \cdot x + 8.7731858$	5.73	8.77	0.98
13	6.0×10^{-2}	$y = 5.4283186 \cdot x + 9.1270796$	5.43	9.13	0.97
14	7.0×10^{-2}	$y = 5.4482301 \cdot x + 9.3245575$	5.45	9.32	0.98
15	8.0×10^{-2}	$y = 5.6415929 \cdot x + 8.9253982$	5.64	8.93	0.97
16	9.0×10^{-2}	$y = 5.4668142 \cdot x + 9.2542035$	5.47	9.25	0.99
17	1.0×10^{-1}	$y = 5.5053097 \cdot x + 9.3813274$	5.51	9.38	0.97
18	2.0×10^{-1}	$y = 6.0243363 \cdot x + 8.2235841$	6.02	8.22	0.98
19	3.0×10^{-1}	$y = 4.9331858 \cdot x + 10.475796$	4.93	10.48	0.93
		Average factor value:	**5.63**	**8.94**	**0.97**
		Final formula:	$U_d = \mathbf{5.63 \cdot d + 8.94}$		

On the basis of the analysis and calculations presented above, relations were determined that can be used to determine the value of the breakdown voltage for contacts made of $W_{70}Cu_{30}$ and $Cu_{75}Cr_{25}$ materials for pressures in the range (3.0×10^{-3} Pa ÷ 3.0×10^{-1} Pa):

$$U_{d(W_{70}Cu_{30})} = 5.63 \cdot d + 8.94, \tag{3}$$

$$U_{d(Cu_{75}Cr_{25})} = 12.49 \cdot d + 1.20, \tag{4}$$

where: U_d is the vacuum breakdown voltage of the insulation system, d is the contact gaps.

If you need to calculate the electric field strength at which a breakdown will occur in an insulating system of this type, use the following relationships:

$$E_{(W_{70}Cu_{30})} = \frac{U_{d(W_{70}Cu_{30})}}{d} = \frac{5.63 \cdot d + 8.94}{d}, \tag{5}$$

Table 3. Calculation of the final pattern of the fitting curve for contact material $Cu_{75}Cr_{25}$

Contact material: $Cu_{75}Cr_{25}$					
Lp.	***p*, Pa**	**Curve fitting pattern**	**A-factor**	**B-factor**	**R^2**
1	3.0×10^{-3}	$y = 12.823009 \cdot x + 0.3457522$	12.82	0.35	0.99
2	4.0×10^{-3}	$y = 12.524336 \cdot x + 0.8635841$	12.52	0.86	0.99
3	5.0×10^{-3}	$y = 12.680088 \cdot x + 0.6525221$	12.68	0.65	0.99
4	6.0×10^{-3}	$y = 12.539823 \cdot x + 1.1449558$	12.54	1.14	0.99
5	7.0×10^{-3}	$y = 12.261947 \cdot x + 1.4354867$	12.26	1.44	0.99
6	8.0×10^{-3}	$y = 12.751327 \cdot x + 0.8328319$	12.75	0.83	0.99
7	9.0×10^{-3}	$y = 12.650000 \cdot x + 0.9850000$	12.65	0.99	0.99
8	1.0×10^{-2}	$y = 12.241593 \cdot x + 1.3453982$	12.24	1.35	0.99
9	2.0×10^{-2}	$y = 12.342920 \cdot x + 1.6832301$	12.34	1.68	0.99
10	3.0×10^{-2}	$y = 12.364159 \cdot x + 1.2685398$	12.36	1.27	0.99
11	4.0×10^{-2}	$y = 12.426106 \cdot x + 1.1740265$	12.43	1.17	0.99
12	5.0×10^{-2}	$y = 12.280973 \cdot x + 1.4977434$	12.28	1.50	0.99
13	6.0×10^{-2}	$y = 12.188938 \cdot x + 1.5947345$	12.19	1.59	0.99
14	7.0×10^{-2}	$y = 12.173894 \cdot x + 1.5459735$	12.17	1.55	0.99
15	8.0×10^{-2}	$y = 12.637611 \cdot x + 1.3119027$	12.64	1.31	0.99
16	9.0×10^{-2}	$y = 12.943805 \cdot x + 0.8884513$	12.94	0.89	0.99
17	1.0×10^{-1}	$y = 12.515487 \cdot x + 1.4913717$	12.52	1.49	0.99
18	2.0×10^{-1}	$y = 12.407965 \cdot x + 1.4969912$	12.41	1.50	0.99
19	3.0×10^{-1}	$y = 12.496018 \cdot x + 1.2465044$	12.50	1.25	0.99
		Average factor value:	**12.49**	**1.20**	**0.99**
		Final formula:	$U_d = 12.49 \cdot d + 1.20$		

$$E_{(Cu_{75}Cr_{25})} = \frac{U_{d(Cu_{75}Cr_{25})}}{d} = \frac{12.49 \cdot d + 1.20}{d}, \tag{6}$$

where E is the electric field strength at which an electric breakdown occurs in a vacuum insulation system.

Using the final formulas of the fitting function developed, the average values of the breakdown voltages in the pressure range (3.0×10^{-3} Pa÷3.0×10^{-1} Pa) seen in Fig. 5(a) and 5(b) were calculated. The calculated values of U_d breakdown voltages are summarized in Table 4.

Comparing the calculated values of U_d breakdown voltages summarized in the table above with the characteristics shown in Figs. 5(a) and 5(b), it can be concluded that the developed fitting function formulas that allow the calculation of U_d breakdown voltages do their job satisfactorily.

Table 4. Calculated average values of breakdown voltages by type of contact material and the value of the contact gap

Contact gaps / Contact material	$W_{70}Cu_{30}$	$Cu_{75}Cr_{25}$
d_1 = 0.7 mm	12.88 kV	9.94 kV
d_2 = 0.9 mm	14.01 kV	12.44 kV
d_3 = 1.5 mm	17.39 kV	19.94 kV
d_4 = 1.7 mm	18.51 kV	22.43 kV
d_5 = 2.3 mm	21.89 kV	29.93 kV
d_6 = 2.7 mm	24.14 kV	34.92 kV

3.2. Effect of residual gas pressure on electrical strength

The next part of the laboratory tests involved measurements of breakdown voltages in a vacuum insulation system with residual gases in the form of air and three noble gases: argon, neon and helium. The tests were performed for four contact gaps: d_1 = 0.7 mm, d_2 = 0.9 mm, d_3 = 1.7 mm, d_4 = 2.3 mm. Characteristics of $U_d = f(p)$ comparing the types of residual gases used for each of the contact gaps $d_1 \div d_4$ are shown in Figs. 8(a)–8(d).

Two characteristic ranges are distinguished on the above characteristics. Below a certain value of residual gas pressure, the electrical strength of the system oscillates at a similar level for each of the analyzed gases. Beyond this value, the insulating properties of the system are lost. The authors of the present study focused on the noticeable differences in the pressure values at which the analyzed vacuum insulating system lost its insulating properties. These values are summarized in Table 5.

Table 5. Calculated average values of breakdown voltages by type of contact material and the value of the contact gap

Residual gas / Contact gap	d_1 = 0.7 mm	d_2 = 0.9 mm	d_3 = 1.7 mm	d_4 = 2.3 mm	Average value
Argon	0.40 Pa	0.30 Pa	0.32 Pa	0.31 Pa	0.33 Pa
Air	0.50 Pa	0.42 Pa	0.38 Pa	0.35 Pa	0.41 Pa
Neon	0.69 Pa	0.69 Pa	0.60 Pa	0.58 Pa	0.64 Pa
Helium	2.60 Pa	2.50 Pa	2.60 Pa	2.50 Pa	2.55 Pa

Analyzing the data presented in the table above, it can be seen that the pressure values of selected residual gases, above which there is a drastic decrease in the measured values of the breakdown voltages, do not depend significantly on the set contact gaps d. The average value of the critical pressure point is, respectively, for argon 0.33 Pa, for air 0.41 Pa, for neon 0.64 Pa, and for helium 2.55 Pa.

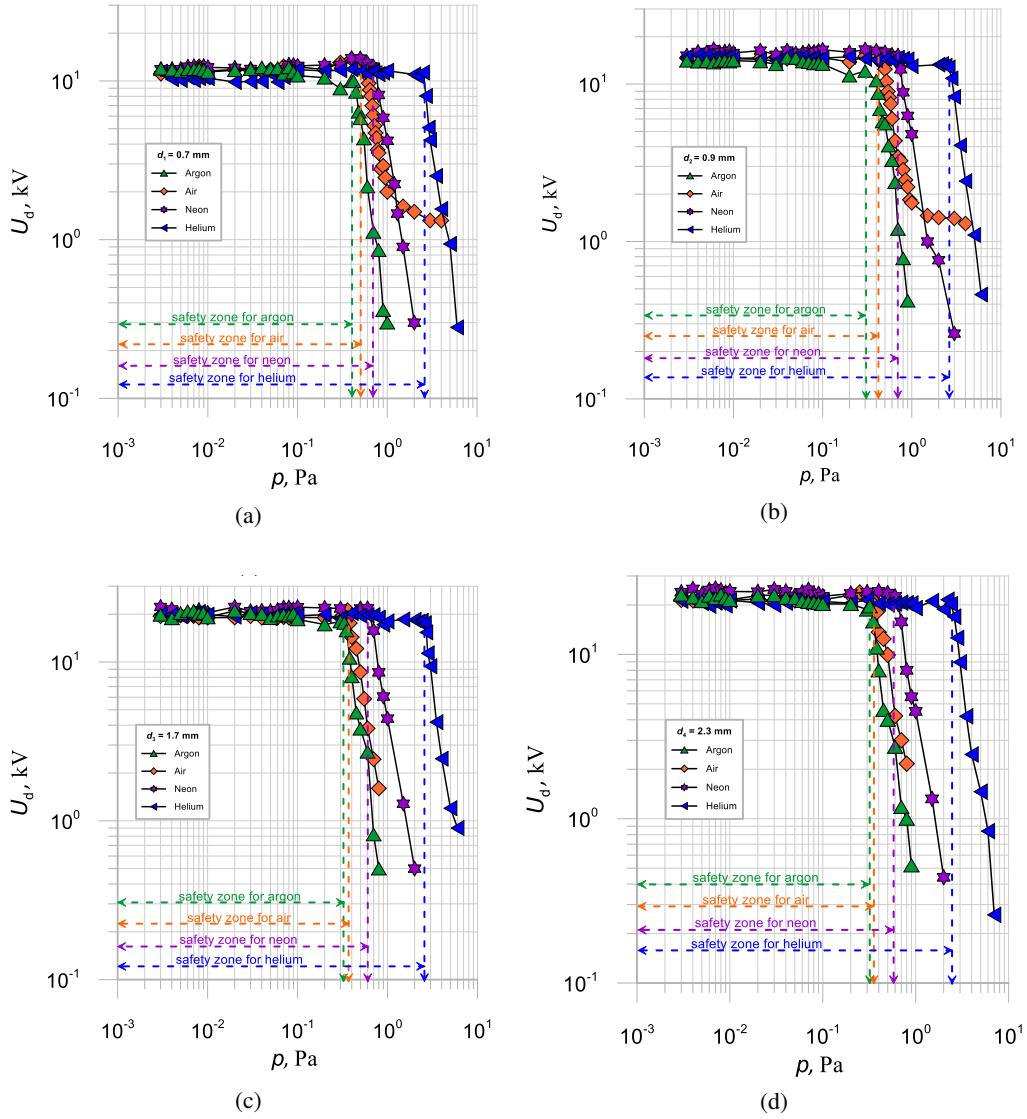

Fig. 8. Dependence of U_d breakdown voltage as a function of pressure p of residual gases in the form of argon, air, neon, and helium for selected values of contact gaps: (a) d_1 = 0.7 mm; (b) d_2 = 0.9 mm; (c) d_3 = 1.7 mm; (d) d_4 = 2.3 mm

Marking in Figs. 8(a)–8(d) the values of the pressures summarized in Table 4, the width of the safety zones formed is evident, which are characterized by the electrical strength of the system keeping U_d constant. The system with residual gases in the form of helium looks the most favorable in this case, while the system with residual gases in the form of argon looks the worst.

4. Conclusions

Due to the increasing demand for electricity, the increase in reliability indices and miniaturization trends, improving the performance of medium- and high-voltage vacuum switching apparatus is an unavoidable need [27]. In this situation, it is necessary to thoroughly understand the phenomenon of the initiation and development of vacuum interrupters used in electric power switching apparatus.

The authors of the present paper carried out a series of measurements of breakdown voltages in the discharge chamber in a system of electrodes with contact pads made of $W_{70}Cu_{30}$ and $Cu_{75}Cr_{25}$ materials and for residual gases in the form of air, argon, neon and helium.

Comparing the contact materials used in the study, it was found that the Cu–Cr material for distances greater than 1 mm is characterized by higher breakdown voltages. Linear functions were determined to estimate the values of this parameter, both for Cu–Cr and W–Cu contacts. Thanks to this, it is possible to determine the parameters of the system supplying the test chamber, or to determine the parameters of the test sample, before proceeding with the tests.

Based on the laboratory measurements obtained, it was found that the discharge chamber with a vacuum obtained on the basis of helium maintains full insulating capacity in the largest pressure range, while in the smallest for a vacuum obtained on the basis of argon. The final value of this interval was 2.55 Pa for helium, 0.64 Pa for neon, 0.41 Pa for air and 0.33 Pa for argon, respectively. The significant differences in the given pressure values are directly related to the ionization energies of these gases, which are discussed in the theoretical part of this article. Taking into account the rated operating pressure of vacuum interrupters used in the electric power industry, which is about 10^{-3} Pa, this provides an opportunity to potentially increase the value of this parameter by using helium or neon as a residual gas in the interrupter. With a higher pressure rating, there is less chance of a potential leakage of the chamber, and thus of a high potential transfer to the other pole of the switching apparatus. This is therefore an opportunity to increase the reliability of electrical equipment, which is in line with current trends in the electric power industry. In addition, the use of this type of insulating medium is completely safe for the environment and upholds the environmental trend of eliminating greenhouse gases from the atmosphere [27–30].

Acknowledgements

This work was supported by The National Centre for Research and Development and co-financed from the European Union funds under the Smart Growth Operational Programme (grant # POIR.01.01.01-00-0451/21).

References

[1] Opydo W., *Properties of Gas and Vacuum High Voltage Insulation Systems* (in Polish), Poznan University of Technology Publishing (2008).

[2] Szpor S., Dzierżek H., Winiarski W., *High Voltage Technology* (in Polish), WNT (1978).

[3] Flisowski Z., *High Voltage Technology* (in Polish), WNT (1999).

[4] Szpor S., *Electrical strength and insulation technology* (in Polish), PWN (1959).

[5] Hałas A., *High Vacuum Technology* (in Polish), PWN (1980).

[6] Van Atta L.C., Van De Graaf R.J., Barton H.A., *A new design for a high – voltage discharge tube*, Phys. Rev., vol. 43, p. 158 (1933), DOI: 10.1103/PhysRev.43.158.

[7] Wijker W.J., *The electrical breakdown in vacuum*, Appl. Sci. Res., vol. 9, p. 1 (1961).

[8] Cranberg L., *The initiation of electrical breakdown in vacuum*, J. Appl. Phys., vol. 23, p. 518 (1952), DOI: 10.1063/1.1702243.

[9] Tarasova L.V., *Desorbcionnyj mehanizm èlektričeskogo proboâ v vakuume*, Doklady AN SSSR, vol. 167, p. 330 (1966).

[10] Flowers P., Theopold K., Langley R., Neth E.J., Robinson W.R., *Chemistry 2e by OpenStax*, Hardcover (2019).

[11] Marić D., Malović G., Petrović Z.L., *Space–time development of lowpressure gas breakdown*, Plasma Sources Sci. Technol., vol. 18, no. 034009 (2009), DOI: 10.1088/0963-0252/18/3/034009.

[12] Fu Y., Yang S., Zou X., Luo H., Wang X., *Effect of distribution of electric field on low-pressure gas breakdown*, Physics of Plasmas, vol. 24, no. 023508 (2017), DOI: 10.1063/1.4976848.

[13] Pejovic M.M., Ristic G.S., Karamarkovic J.P., *Electrical breakdown in low pressure gases*, Journal of Physics D: Applied Physics, vol. 35, pp. 91–103 (2002), DOI: 10.1088/0022-3727/35/10/201.

[14] Lisovskiy V.A., Osmayev R., Gapon A., Dudin S., Lesnik I., Yegorenkov V., *Electric field non-uniformity effect on dc low pressure gas breakdown between flat electrodes*, Vacuum, vol. 145, pp. 19–29 (2017), DOI: 10.1016/j.vacuum.2017.08.022.

[15] Hou C. *et al*., *W–Cu composites with submicron- and nanostructures: progress and challenges*, NPG Asia Materials, vol. 11, no. 74 (2019), DOI: 10.1038/s41427-019-0179-x.

[16] Dong L.L., Ahangarkani M., Chen W.G., Zhang Y.S., *Recent progress in development of tungsten-copper composites: fabrication, modification and applications*, Int. J. Refract. Met. Hard Mater., vol. 75, pp. 30–42 (2018), DOI: 10.1016/j.ijrmhm.2018.03.014.

[17] Fan J.L., Peng S.G., Liu T., Cheng H.C., *Application and research status of W–Cu composite materials*, Rare Met. Cem. Carbides, vol. 34, no. 3, pp. 30–35 (2006).

[18] Chen W., Dong L., Zhang Z. *et al*., *Investigation and analysis of arc ablation on WCu electrical contact materials*, J. Mater. Sci.: Mater. Electron., vol. 27, pp. 5584–5591 (2016), DOI: 10.1007/s10854-016-4463-z.

[19] Bukhanovsky V.V., Grechanyuk N.I., Minakova R.V. *et al*., *Production technology, structure and properties of Cu–W layered composite condensed materials for electrical contacts*, Int. J. Refract. Met. Hard Mater, vol. 29, no. 5, pp. 573−581 (2011), DOI: 10.1016/j.ijrmhm.2011.03.007.

[20] Jiang G.S., Wang Z.F., Yi G., *Impact on the tungsten copper electronic packaging materials microstructure and properties of high-temperature forging*, Powder Metall. Mater. Sci. Eng., vol. 16, no. 3, pp. 403–406 (2011).

[21] Wei X., Wang J., Yang Z., Sun Z., Yu D., Song X., Ding B., Yang S., *Liquid phase separation of Cu–Cr alloys during the vacuum breakdown*, Journal of Alloys and Compounds, vol. 509, pp. 7116–7120 (2011), DOI: 10.1016/j.jallcom.2011.04.017.

[22] Zhai X., Xiao W., Mudi K., Ruan X., *Effect of Powder Form and SPS Process Sintering on CuCr50 Alloy Powder*, Proceedings of the 2015 International Conference on Mechatronics, Electronic, Industrial and Control Engineering, Shenyang, China, pp. 88–91 (2015), DOI: 10.2991/meic-15.2015.22.

[23] Wanga L., Zhang X., Wang Y., Yang Z., Jia S., *Simulation of cathode spot crater formation and development on CuCr alloy in vacuum arc*, Physics of Plasmas, vol. 25, no. 043511 (2018), DOI: 10.1063/1.5023213.

[24] Mostic D., Osmokrovic P., Stankovic K., Radosavljevi R., *Dielectric characteristics of vacuum circuit breakers with CuCr and CuBi contacts before and after short-circuit breaking operations*, Vacuum, vol. 86, no. 2, pp. 156–164 (2011), DOI: 10.1016/j.vacuum.2011.05.007.

[25] Osmokrovic P., Vujisic M., Stankovic K., Vasic A., Loncar B., *Mechanism of electrical breakdown of gases for pressures from 10^{-9} to 1 bar and inter-electrode gaps from 0.1 to 0.5 mm*, Plasma Sources Sci. Technol., vol. 16, no. 643 (2007), DOI: 10.1088/0963-0252/16/3/025.

[26] Lech M., Węgierek P., *Breakdown Initiation and Electrical Strength of a Vacuum Insulating System in the Environment of Selected Noble Gases at AC Voltage*, Energies, vol. 15, no. 1154 (2022), DOI: 10.3390/en15031154.

[27] *Power engineering, distribution and transmission*, Polish Power Transmission and Distribution Association's Report, Poznań (2021).

[28] Węgierek P., Lech M., Kostyła D., Kozak C., *Study on the Effect of Helium on the Dielectric Strength of Medium-Voltage Vacuum Interrupters*, Energies, vol. 14, no. 3742 (2021), DOI: 10.3390/en14133742.

[29] Slade P.G., *The Vacuum Interrupter Theory, Design, and Application*, CRC Press (2021).

[30] Regulation (EU) No. 517/2014 of the European Parliament and of the Council on fluorinated greenhouse gases of 16 April 2014.